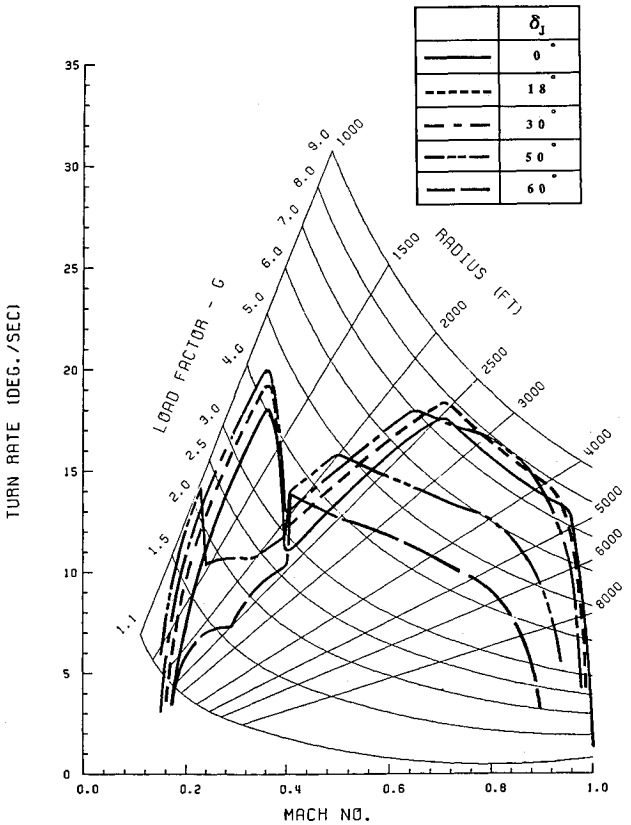

Fig. 2 Effect of thrust vectoring on sustained level-turn performance for a fighter aircraft (Altitude = 5000 ft, W = 10,000 lb, and sea-level thrust = 2 × 5000 lb).

minimum radius of turn is equal to 1670 ft with $\delta_j = 0$ at low speeds and is 1420 ft at an optimal $\delta_j = 45$ deg. It should be noted the n_{max} and ψ_{max} with thrust vectoring tend to occur at a lower Mach number than that without thrust vectoring.

***T/W* = 1.0**

The results are presented in Fig. 2. It is seen that without thrust vectoring, $n_{max} = 7.47$ at $M = 0.82$, $\psi_{max} = 17.5$ deg/s at $M = 0.71$ and $R_{min} = 1250$ ft at low speeds. With thrust vectoring, $n_{max} = 7.95$ at $M = 0.82$ and an optimal $\delta_j = 30$ deg; $\psi_{max} = 18.4$ deg/s at $M = 0.71$ and an optimal $\delta_j = 18$ deg; and finally, $R_{min} = 1020$ ft with an optimal $\delta_j = 50$ deg. These results represent a gain of 6% for n_{max} and 5% for ψ_{max}.

As shown in the above results, the performance gain in level turn due to thrust vectoring depends not only on the basic airplane aerodynamics (e.g., C_{Do}, k, C_{LB}, C_{Lmax}), but also on the available thrust-weight ratio as well as the structural limit load factor. However, the calculated performance gain is much less than that indicated in Ref. 4. In the latter, it was shown in descending turns that thrust vectoring provided about 20% improvement in turning time at high initial speeds. At low initial speeds, the improvement was small. This significant improvement in performance due to thrust vectoring is most likely the result of assuming a constant maximum aerodynamic load factor and ignoring compressibility effect on drag at high speeds. Therefore, more thrust can be utilized to augment the aircraft lift so that the turn rate is increased. In the present analysis, the maximum aerodynamic load factor is mostly limited by the buffet lift coefficients that decrease with Mach number. The effect of compressibility on C_{Do} and k has also been included by using the experimental data. Another difference is sustained performance being considered in the present analysis and instantaneous performance in Ref. 4.

Conclusions

A method of analysis was presented to determine the effect of thrust vectoring on level-turn performance. Calculated results based on the basic F-5E aerodynamics were presented. It was shown that different optimal thrust deflection angles existed for the sustained maximum load factor, turn rate, and minimum turn radius. Gains in maximum load factor and turn rate due to thrust vectoring were 2% and 3%, respectively, at a thrust-weight ratio of 0.77 at 5000-ft altitude. However, the corresponding gains were increased to 6% and 5% at a thrust-weight ratio of 1.0.

References

[1]Mason, M. L., and Burley, J. R., III, "Static Investigation of Two STOL Nozzle Concepts with Pitch Thrust-Vectoring Capability," NASA TP-2559, April 1986.

[2]Berrier, B. L., and Mason, M. L., "A Static Investigation of Yaw Vectoring Concepts on Two-Dimensional Convergent-Divergent Nozzles," AIAA Paper 83-1288, Seattle, WA, June 1983.

[3]Miller, E. H., "Performance of a Forward Swept Wing Fighter Utilizing Thrust Vectoring and Reversing," *Journal of Aircraft*, Vol. 23, No. 1, 1986, pp. 68–75.

[4]Schneider, G. L., and Watt, G. W., "Minimum-Time Turns Using Vectored Thrust," *Journal of Guidance, Control, and Dynamics*, Vol. 12, No. 12, 1989, pp. 777–782.

[5]Lan, C. E., and Roskam, J., *Airplane Aerodynamics and Performance*, Roskam Aviation and Engineering Corp., Ottawa, KS, 1988, p. 493.

[6]Paulson, J. W., Jr., et al., "A Review of Technologies Applicable to Low-Speed Flight of High-Performance Aircraft Investigated in the Langley 14×22-ft Subsonic Tunnel," NASA TP-2796, May 1988.

Transition of the Flutter Mode of a Two-Dimensional Section with an External Store

Zhi-chun Yang* and Ling-cheng Zhao†
Northwestern Polytechnical University, Xi'an, People's Republic of China

RECENTLY, Niblett[1] made a comprehensive study of the classical bending-torsion flutter, in which the flutter condition was related directly to the normal modes involved in flutter.

By using normalized eigenmodes and steady aerodynamics, the equation of motion of a wing is

$$\begin{bmatrix} 1 & \\ & 1 \end{bmatrix} \begin{bmatrix} \ddot{\xi}_i \\ \ddot{\xi}_j \end{bmatrix} + \begin{bmatrix} \omega_i^2 & \\ & \omega_j^2 \end{bmatrix} \begin{bmatrix} \xi_i \\ \xi_j \end{bmatrix} = \begin{bmatrix} c_{ii}q & c_{ij}q \\ c_{ji}q & c_{jj}q \end{bmatrix} \begin{bmatrix} \xi_i \\ \xi_j \end{bmatrix} \quad (1)$$

where ξ_i and ξ_j are the normal coordinates; ω_i and ω_j are the ith and jth eigenfrequencies, $\omega_i < \omega_j$, q is the dynamic pressure, and c_{ij} is the generalized aerodynamic coefficient obtained from the virtual work principle as

$$qc_{ij} = z_i L_j \quad (2)$$

with

L_j = the lift force associated with the jth mode

z_i = vertical displacement of the aerodyamic center associated with the ith mode

An explicit formula for the lower flutter critical dynamic

Received Nov. 15, 1989; revision received Oct. 15, 1990; accepted for publication March 27, 1991.

*Research Associate, Aircraft Engineering Department.
†Professor, Aircraft Engineering Department.

pressure is obtained as

$$q_{cr} = (\omega_j^2 - \omega_i^2)/(c_{jj} - c_{ii} + 2\sqrt{-c_{jj}c_{ii}}) \tag{3}$$

where the relation $c_{ij}c_{ji} = c_{jj}c_{ii}$ has been used.

The existence of flutter is warranted by a real and positive value of q_{cr}, for which the necessary and sufficient condition is

$$c_{ii} < 0 \quad \text{and} \quad c_{jj} > 0 \tag{4}$$

By referring to mode shapes shown in Fig. 1, with $\alpha_i > 0$, $\alpha_j > 0$, hence $L_i > 0$, $L_j > 0$, and the flutter condition (4) is equivalent to

$$z_i < 0 \quad \text{and} \quad z_j > 0 \tag{5}$$

where α_i and α_j are the angle of attack in ith and jth modes.

The node of the higher order mode is on the downstream side of the aerodynamic center whereas the node of the lower order mode is on the upstream side as shown in Fig. 1.

The conclusion of Ref. 1 may serve as an engineering guide to classical flutter analysis. It may also give useful interpretation to the mode transition problem of wing-store flutter. In the wing-store flutter analysis of Ref. 2, we found that for most cases, only two normal modes have predominant effects and a binary calculation using those two modes could give satisfactory results of flutter speed.

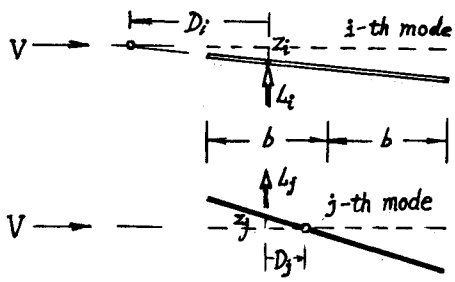

Fig. 1 Sketch of the normal modes.

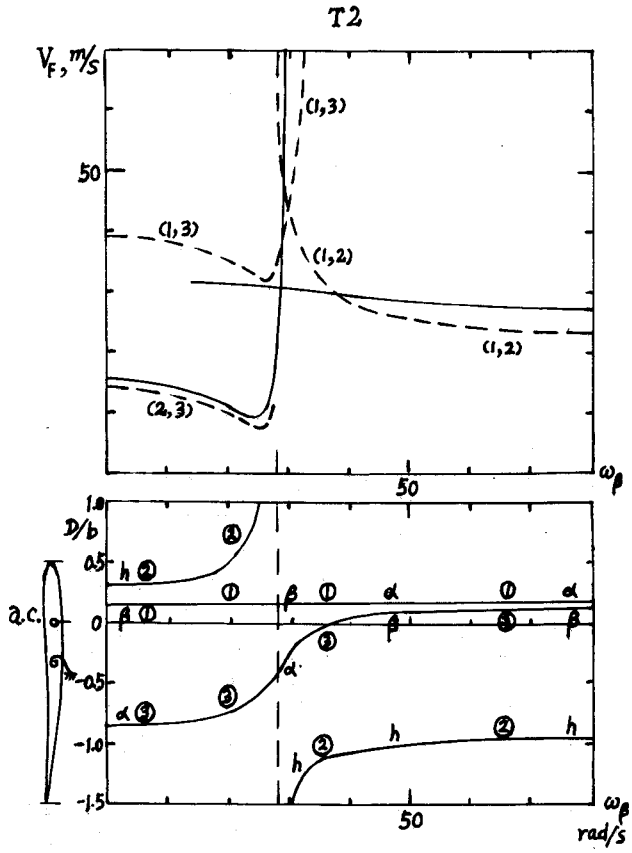

Fig. 2 Flutter boundary and node position of normal modes for example T2 from Ref. 2.

Basing upon Niblett's concept, we have made the flutter calculation for all of the examples of Ref. 2, with each two mode binary system (in total three such systems for one example), and have obtained the flutter boundary depicting the change of flutter speed vs store pitching stiffness ω_β. For most examples, the results of the binary frequency coalescence analysis show a variation trend comparable to the exact results of Ref. 2. Especially for the intersection of the two flutter branches, where the sudden change of flutter mode occurs, the frequency coalescence calculation can give a reasonable guide.

The results of the example T2 from Ref. 2 are shown in Fig. 2 in which the dotted line is the frequency coalescence result, whereas solid line represents the exact result. The distance D of the node ahead of aerodynamic center is referred to semichord b, and the variation of D/b of the three normal modes vs ω_β is also shown in Fig. 2, which gives a direct explanation of the cusp of the flutter boundary. For low ω_β, the nodes of the first (store pitching) mode and the second (wing heave) mode are both on the upstream side whereas the node of the third (wing torsion) mode is on the downstream side of the aerodynamic center. Hence, the first-third mode coupled flutter, denoted by (1,3)-flutter, as well as the (2,3)-flutter exist. From Eq. (3), we have

$$q_{(1,3)} = (\omega_3^2 - \omega_1^2)/(c_{33} - c_{11} + 2\sqrt{-c_{33}c_{11}})$$

$$q_{(2,3)} = (\omega_3^2 - \omega_2^2)/(c_{33} - c_{22} + 2\sqrt{-c_{33}c_{22}}) \tag{6}$$

Since for low ω_β the first mode is a store-pitching dominant mode in which the wing motion is rather small, therefore L_1 and z_1, hence c_{11}, are very small so $|c_{11}| << |c_{22}|$. Thus $q_{(1,3)}$ has a smaller denominator and a larger numerator than $q_{(2,3)}$ and is greater than $q_{(2,3)}$. So in the low ω_β range, the coupled second and third modes constitute the flutter boundary.

Along with increasing ω_β, the node of second mode moves upstream to infinity, and for ω_β just over 28 rad/s, it suddenly jumps to downstream infinity. At this critical ω_β the second mode becomes pure heave mode. Since for $\omega_\beta > 28$ rad/s the nodes of the second and third modes are on the same downstream side, they cease to induce coupled (2,3)-flutter. For ω_β still increasing to 37 rad/s, the node of third mode moves forward across the aerodynamic center, then the (1,3)-flutter also vanishes. There remains only the possibility of (1,2)-flutter, which represents the flutter boundary in the high ω_β range. In general, the critical ω_β^* at which pure heave mode occurs can be determined by the following equation

$$\omega_\beta^* = \omega_h \sqrt{\frac{\mu_h}{m_{33}} \left(\frac{m_{23}(m_{33}m_{12} - m_{13}m_{23})}{m_{12}(m_{11}m_{23} - m_{13}m_{22})} \right)} \tag{7}$$

where the meaning of μ_h, ω_h, and m_{ij} are the same as in Ref. 2.

The previous example shows how Niblett's concept provides an engineering guide to identify the constitution of wing-store flutter mode and its transition. The prerequisite information is only the normal mode shapes, which are the direct results of ground vibration test or routine vibration analysis.

References

[1]Niblett, L. T., "A Guide to Classical Flutter," *Aeronautical Journal*, Vol. 92, No. 919, 1988, pp. 339–354.

[2]Yang, Z. C., and Zhao, L. C., "Wing-store Flutter Analysis of an Airfoil in Incompressible Flow," *Journal of Aircraft*, Vol. 26, No. 6, 1989, pp. 583–587.